

Computer Modeling and Measurement of Extended Technical Magnetic Field

Miroslav Novák¹⁾, Martin Truhlář¹⁾, Lubomír Slavík¹⁾ and Miloslav Košek³⁾

¹⁾ Department of Mechatronics and Technical Informatics, Technical University of Liberec, Liberec, Czech Republic, e-mail: *miroslav.novak@tul.cz, martin.truhlar@tul.cz, lubomir.slavik@tul.cz, miloslav.kosek@tul.cz*

Abstract — A personal computer was used for both the measurement and modeling of technical magnetic fields in different areas. The field modeling uses basic physical laws from magnetism in the integral form and is performed by the numeric integration in MATLAB. The apparatus is able to measure a relatively low magnetic field. Important results are presented for the measurement of the DC field in the electromagnetic flow meter and AC field in the distribution point. Only simple models were applied, nevertheless the agreement with the experiment is good. Deviations are due to inaccuracies both in the production and experiment, predominantly. Their sources are not simple models. Therefore, the models are applicable for reliable design or analysis of devices using magnetic field.

Keywords — Computer simulation, computer controlled experiment, magnetic field modeling, Biot-Savart Law, electromagnetic flow meter, power distribution point, skin-effect

I. INTRODUCTION

Magnetic field interactions are used in many technical areas, for instance strong field in a small area are necessary for contact-less force action [1] and spatially extended field performs forces on charged moving particles in the electromagnetic flow meter [2]. In the design and analysis of such devices the magnetic field should be known. As the structure of the devices is complicated, approximated models are used and calculations are made numerically. Therefore, the experimental verification of the models is necessary.

Another reason of the magnetic field modeling is to examine magnetic fields generated by strong currents. Typical example is the distribution point [3]. Strong currents that flow in distribution points, can lead to high forces between conductors, especially when transition effects take a place. In order to estimate the forces, the magnetic field produced by the conductors must be known. It can be calculated from currents in the conductors, but the calculation must be verified experimentally, at least in the initial stage of the research.

Because of high currents, distribution points use conductors of a large cross section. Due to the skin effect, the current density is not uniform in them even at low technical frequencies. In this simple case the current distribution can be approximated by an analytical form and calculated simply. Unfortunately, the solution is in an unusual complex symbolic form. Its understanding is more difficult and its improper use can lead to serious errors. Therefore, the experimental verification of the results is again necessary. Since the current density inside the conductor cannot be measured, its theoretical distribution should be verified by an excited magnetic

field. It is the second, theoretical, reason for the magnetic field precise measurement.

Other specific areas of the magnetic field modeling are calculations of magnetically coupled circuit parameters, mutual and self inductance. Last but not least, a very complicated application is the modeling of generation of ultrasound by Lorentz force excited by a special coil.

These typical and many other special technical problems show that the perfect modeling of the magnetic field produced by both the DC and AC excitation currents is necessary. The verification of models needs a perfect experiment. In the paper a relatively general method for both the DC and AC magnetic field modeling is presented and the robust experiment for the verification of the models is shown.

II. THEORY

The modeling technique is based on the Biot-Savart Law that is a general formula for the magnetic field calculation. We present it in a typical form for a line current I flowing in a very thin conductor given by the curve K . The magnetic flux density $\vec{B}(\vec{r})$ in a point of the position vector is given by the formula (Biot-Savart Law)

$$\vec{B}(\vec{r}) = \frac{\mu_0}{4\pi} I \int_{(K)} \frac{\vec{t}_0 \times (\vec{r} - \vec{r}_0)}{|\vec{r} - \vec{r}_0|^3} dl, \quad (1)$$

where $\vec{t}_0 = \vec{t}_0(\vec{r}_0)$ is the unit vector tangential to the curve K in the point with the position vector \vec{r}_0 , where is the conductor element dl . The sense of the unit vector \vec{t}_0 is given by the current I sense. The universal constant μ_0 is the permeability of vacuum.

This form of the Biot-Savart Law is used frequently for calculation of the magnetic flux density generated by technical coils. Other practical forms of the Biot-Savart Law are for the plane and volume currents, if they cannot be approximated by line ones. The exciting quantity is the surface or volume current density, respectively. The integration is performed along a given plane or a given volume, respectively. The formulae can be found in every textbook.

Analytical solutions of (1) are known for special cases only. Typical example is the magnetic flux density on the axis of a circular loop. However, for this paper a straight thin conductor is important. Let us consider that the conductor is parallel to the Z axis and its coordinate z_0 changes from $-L$ to $+L$. The conductor intersects the plane XY at a point of the coordinates (x_d, y_d) . The integration of formula (1) for this case leads to this formula, known from

literature [4], for instance, for all components of the magnetic flux density

$$B_x(x, y, z) = \frac{\mu_0 I}{4\pi} \frac{y - y_d}{(x - x_d)^2 + (y - y_d)^2} \left[\frac{z - L}{\sqrt{(z - L)^2 + K_{xy}}} - \frac{z + L}{\sqrt{(z + L)^2 + K_{xy}}} \right]$$

$$B_y(x, y, z) = \frac{-\mu_0 I}{4\pi} \frac{x - x_d}{(x - x_d)^2 + (y - y_d)^2} \left[\frac{z - L}{\sqrt{(z - L)^2 + K_{xy}}} - \frac{z + L}{\sqrt{(z + L)^2 + K_{xy}}} \right]$$

$$B_z(x, y, z) = 0 \quad , \quad (2)$$

where

$$K_{xy} = (x - x_d)^2 + (y - y_d)^2$$

If DC excitation is used, the current density in conductors of a large cross section is uniform. In the case of the AC excitation two other well-known effects take a place: skin-effect and eddy currents. Their result is a non-uniform current density in massive conductors.

As for the eddy currents, the problem is very complicated and probably no simple analytical formula exists. On the other hand, in the case of skin-effect well-known theoretical formulae exist for half-space, infinite layer and infinite conductor of a circular cross section. We derived an approximated formula [3] for the electric field (and therefore also for current density) in the conductor of a rectangular cross section of the length $2a$ along X axis and of the height $2b$ in the direction of Y axis

$$E_0(x, y) = E_0 \left[\begin{array}{l} -\frac{\cosh(\hat{\delta}x)\cosh(\hat{\delta}y)}{\cosh(\hat{\delta}a)\cosh(\hat{\delta}b)} + \\ + \frac{\cosh(\hat{\delta}x)}{2\cosh(\hat{\delta}a)} + \frac{\cosh(\hat{\delta}y)}{2\cosh(\hat{\delta}b)} \end{array} \right] \quad (3)$$

where the complex attenuation constant is given by the formula

$$\hat{\delta} = (1 + j) \sqrt{\frac{\omega\mu\gamma}{2}}$$

where ω is angular frequency, μ is permeability of the conductor material and γ is its electrical conductance.

Main complication is in the fact that formula (3) is the approximate solution of equations for skin-effect, but in the complex form; therefore the electric field strength (3) is of no physical meaning. In the symbolic calculus used in the circuit theory physical meaning has real or imaginary part. Therefore, the skin-effect can be included into calculations, if the real part of (3) is used in formulae like (2) and the current I is replaced by the current density i in a given point of the conductor cross section.

III. EXPERIMENT

Since the plane measurement of the magnetic field is required, the apparatus must be fully automated, because

of a big number of the measured points. The basic block schema of the realized apparatus is in Fig. 1 intended to the study of the flow meter magnetic field. A space positioning system controlled by the computer is used for the probe movement, the probe data are digitalized, noise and unwanted signals are rejected (or reduced) digitally and then all the important data are stored in the computer memory for further processing. The probe movement can be controlled either automatically or individually.

The realized apparatus for the flow meter magnetic field study is in Fig. 2. The symbols are the same as for the universal block schema in Fig. 1.

A detailed photograph of the inner part of the flow meter, after removing the screening, is in Fig. 3. Excitation coils are well visible.

Total measurement accuracy is given both by the probe and positioning system. Three dimensional (3D) commercial Hall probe was used for the magnetic field measurement. Main problem is to increase the commercial probe sensitivity and save its relative accuracy also for low values. The solution is described elsewhere [5].

The second limitation of total measurement accuracy is the Hall probe position. The relative position can be made of good accuracy thanks to step motors. The only problem is to determine or check the position of the reference point. One solution is the individual movement of the Hall probe into a point of the specific flux density vector. For instance, in the flow meter center of symmetry only one flux density component is non zero, theoretically.

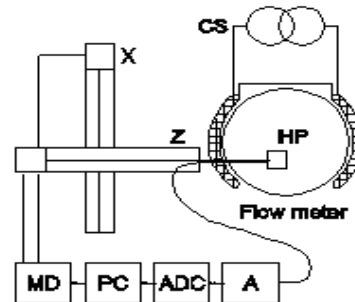


Fig. 1. General apparatus block schema. Legend: FM flow meter, CS current source, Z and X feed axes, HP Hall probe, A signal conditioning, ADC analogue to digital converter, PC personal computer, MD motor driver.

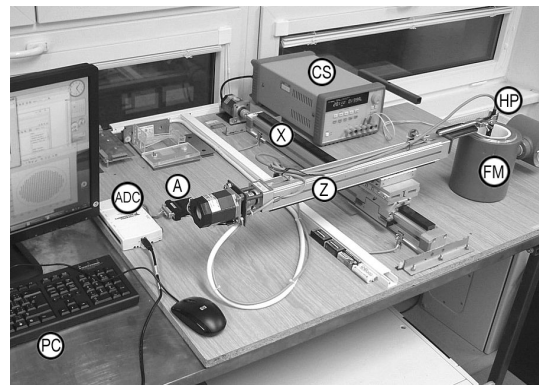


Fig. 2. Photograph of apparatus. Explanation of symbols is in Fig. 1.



Fig. 3. Photograph of flow meter inner part.

Individual probe moving was realized by use of the computer control panel shown in Fig. 4. General plane movement is performed by mouse clicking. The probe position and measured flux density are continuously displayed.

The second series of fairly different measurements were made in the power distribution net. The photograph of experimental arrangement is in Fig. 5. The distribution net was experimentally modeled by three parallel massive conductors connected to a three phase system via transformers. The conductors are star connected

The measurement of the flow meter was made predominantly in the DC regime although some AC data are also available. On the other hand the second series of measurement for the power distribution net can be made only in an AC excitation. In both cases the flux density is relatively low of an order of 1 mT or less, therefore the effect of noise and other disturbing signals makes a serious problem.

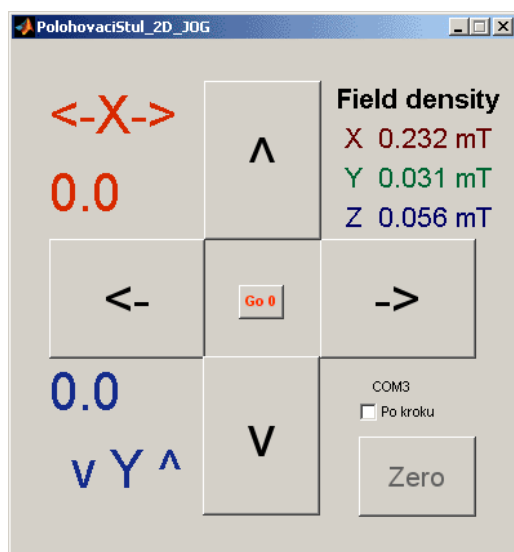


Fig. 4. Computer control panel for probe motion performed individually.

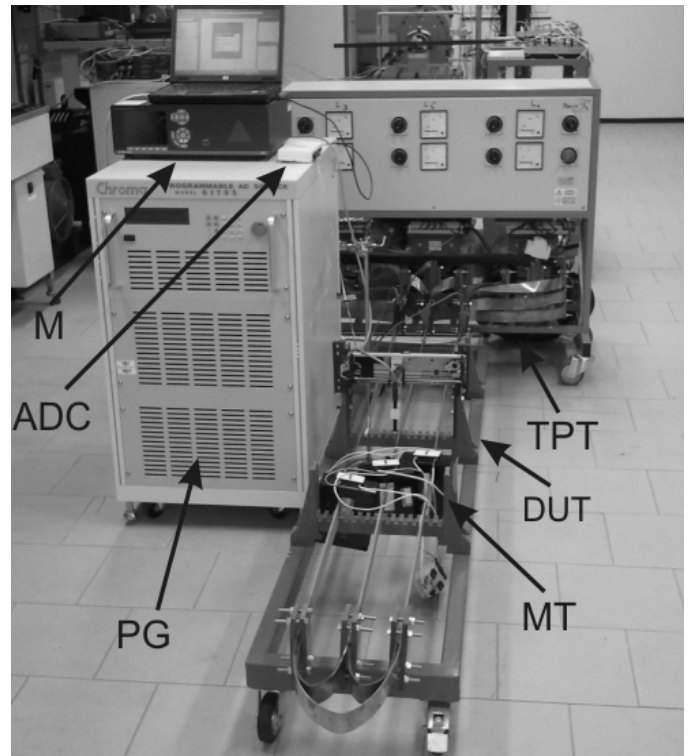


Fig. 5. Apparatus for the complete power distribution net study.
Legend: PG – Power generator Chroma 61704, M – General purpose meter Norma 5000, ADC – Analogue to digital converter NiDaq, TPT – Three-phase transformer, DUT – Massive conductors, MT – Measuring transformers.

IV. DATA PROCESSING AND SIMULATION

Main task in the experimental data processing is to eliminate the noise and other unwanted signals. A typical unwanted signal is the one that comes from the 50 Hz mains. A lot of methods for the noise reduction exist, but some of them may appear to be less effective. All the data processing is made in MATLAB.

A big advantage of the DC regime is easy elimination of noise by averaging. The reduction of the unwanted signal by 40 dB needs averaging through 35 periods. In the case of the AC measurement the application of the Fast Fourier Transform (FFT) was simple and effective.

The calculation of the magnetic field was made in MATLAB. Base for the calculation is the Biot-Savart Law (1) and formula (2). In both cases the numerical integration is used. If the skin-effect is considered, formula (3) was used for the current density distribution in the massive conductor.

For simple models of the flow meter or distribution net the MATLAB itself is satisfactorily fast. If the model refinement is necessary, the computational speed can be increased by parallel computing. A standard four core processor increases speed approximately 4 times that was acceptable in many cases. For very complicated structures the use of the working station is planned.

V. RESULTS

A lot of measurements was made for both investigated devices: flow meter and distribution point. Only basic, important or interesting results will be presented here.

Verification measurements were made under the simplest experimental conditions in order to ensure a good agreement between the experiment and simple model. The presented results are divided into two parts: flow meter results and skin-effect measurement.

A. Flow meter results

In the case of the flow meter the outer screening made from a iron tube complicates the magnetic field inside the tube. Therefore, the first experiments were made with coils glued on a plastic tube. In the plane of symmetry (or mirror plane) perpendicular to the axial axis only the axial component B_y should be non-zero. Parasitic component B_x should have zero value. The coordinate system of the flow meter is defined by Fig. 1, the axial axis is the coordinate Y .

The main component along the diameter in the mirror plane is in Fig. 6. The agreement between experiment and model is good, especially if we take into account that there is a low flux density of an order of 1 mT.

Experimental points in Fig. 6 are not symmetrical, a small asymmetry is evident. It can be explained by production inaccuracy, the coils are not positioned perfectly symmetrically. We can simulate the coil asymmetry in the model by the method of trials and errors. The final result is in Fig. 7. The rotation of one coil in the model by the angle of 1.5° makes much better agreement between the experiment and model.

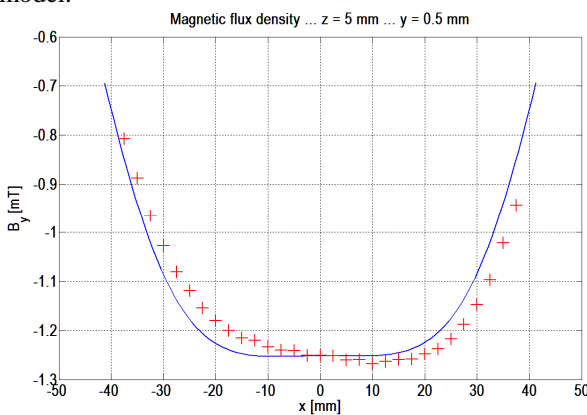


Fig. 6. Main component of the flux density in the flow meter along the diameter in mirror plane.

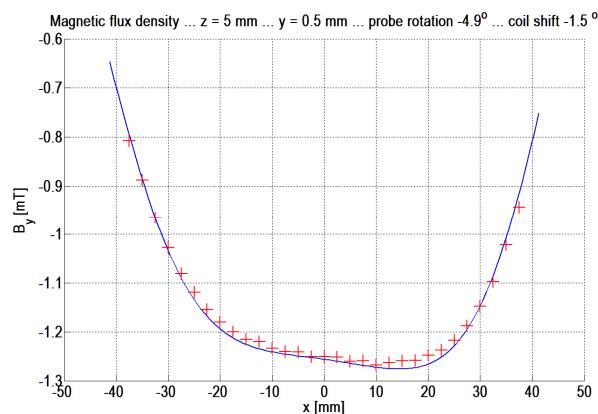


Fig. 7. Effect of a very small asymmetry in the coil position.

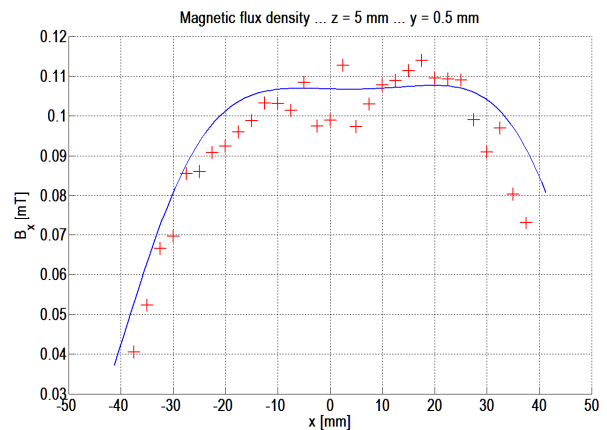


Fig. 8. Parasitic component of the flux density in the flow meter along the diameter in a plane very close to the mirror plane.

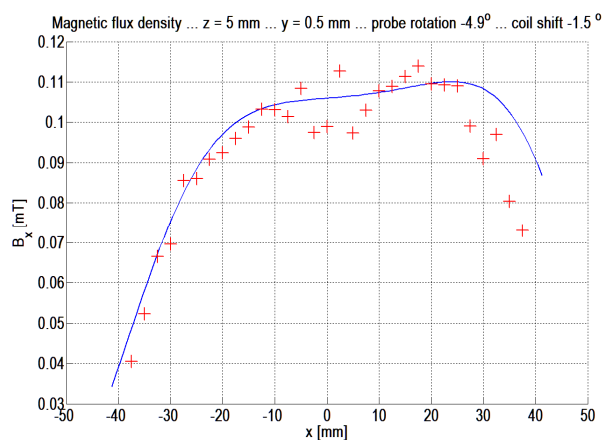


Fig. 9. Effect of a very small asymmetry in the coil position and small probe rotation along its axis.

Comparison of the measured parasitic components and the result from the model for a plane that is very close to the mirror one is in Fig. 8. The agreement between model and experiment is only qualitative.

However, if we take into account the production inaccuracy as in the previous case and add an effect of small probe rotation along its axis, as the experimental inaccuracy, we obtain results that are in Fig. 9. The improvement is visible. We can conclude from Fig. 6 to 9 that the agreement between the model and experiment can be considered as very good, if we take into account very low flux density of an order of 0.1 mT. The field in the flow meter is only two times stronger than the earth magnetic field.

So far presented results were for the worst case in order to present the apparatus and model possibility. A standard measurement on a standard device (with screening wall) along the circle close to the flow meter wall and in the plane positioned at the 20 mm distance from the mirror one is presented in Fig. 10 for main component and in Fig. 11 for the parasitic component. The parasitic component is now the flux density B_z , since the plane is at a relatively great distance from the mirror one. The value of this component is relatively high.

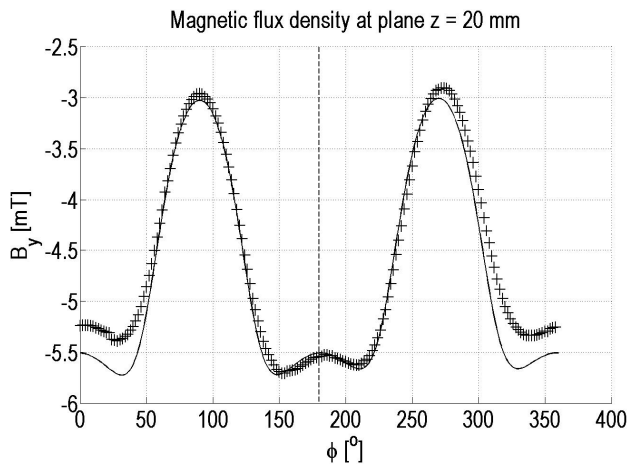


Fig. 10. Main component of the flux density in the complete flow meter along a circle close to the wall.

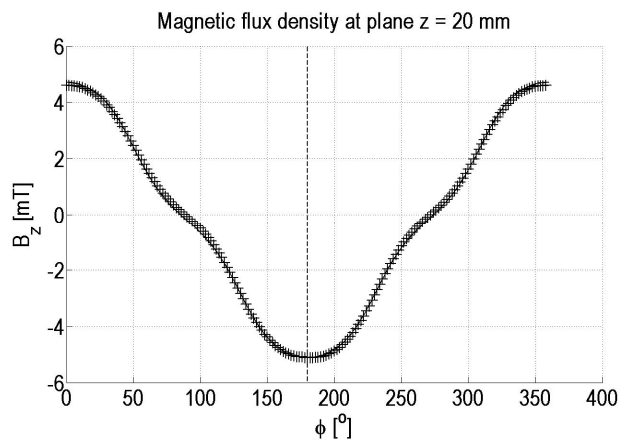


Fig. 11. Parasitic component of the flux density B_z in the complete flow meter along a circle close to the wall.

The flow meter screening steel wall must be reflected in its model. Magnetization of the wall increases the field inside the flow meter. The simplest model for magnetization was used; bounded currents in the screen that are in mirror position to the exciting ones. Their values were found by the method of trials and errors. The agreement between the model and experiment is good, if we consider the simplicity of the model.

In the complete flow meter results the asymmetry of the experimental points is visible in Fig. 10. It can be again explained by a small production inaccuracy. The agreement between very simple model and experiment for the z component of the magnetic flux density in Fig. 11 is almost perfect.

B. Skin effect measurements

The skin effect was studied in the three phase arrangement, according to Fig. 5, but only the central conductor was active. In order to avoid eddy currents, the reference time was at the maximum of the exciting current. Since eddy currents are proportional to the time derivative of the exciting current, at this moment the eddy currents are not generated, theoretically.

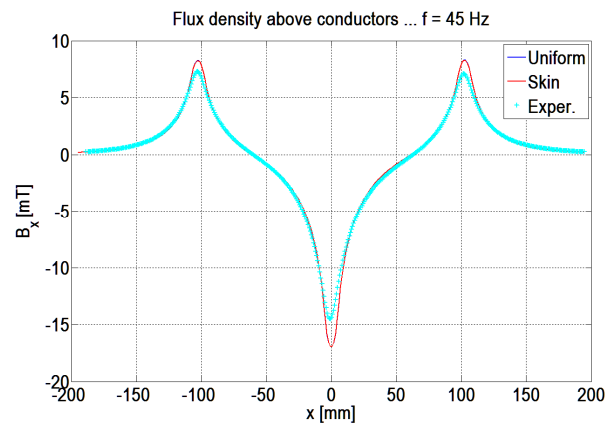


Fig. 12. The magnetic flux density B_x above conductors in the distribution net at a low frequency.

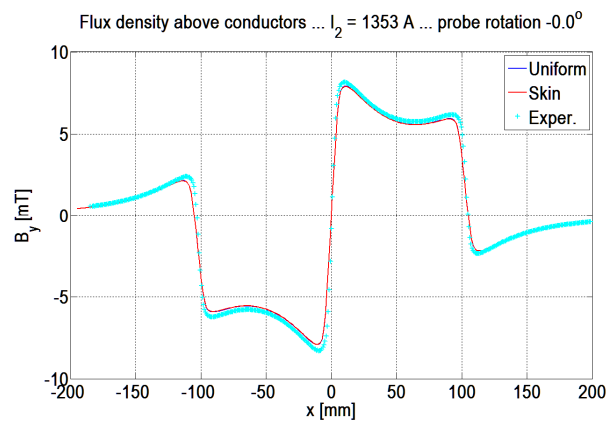


Fig. 13. The magnetic flux density B_y above conductors in the distribution net at a low frequency.

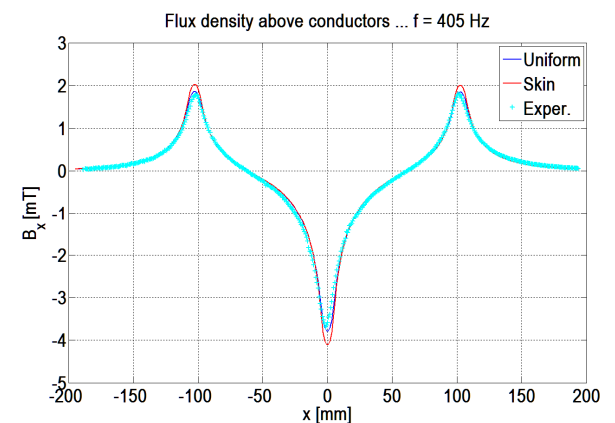


Fig. 14. The magnetic flux density B_x above conductors at a higher frequency of 435 Hz.

Comparison between the model and experiment for one phase distribution net is in Fig. 12 and 13 for both components of the flux density. The probe moves on a line very close to the upper surface of the conductors. The excitation frequency is 45 Hz. In this case the skin effect is negligible and agreement between the experiment and model is good. Small deviations are only at the conductor

edges. Also integrating effect of the probe finite dimensions can be used for the explanation of deviations near extremes in Fig. 12.

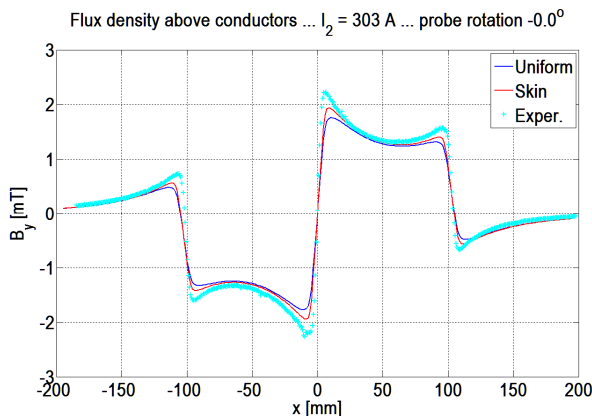


Fig. 15. The magnetic flux density B_y above conductors at higher excitation frequency of 435 Hz.

For frequencies 10 times higher the results are in Fig. 14 and 15. The effect of skin effect is evident only for the y component of the flux density in Fig. 15. Experimental points are close to the model curve for skin effect. The influence of skin effect is confirmed, but the agreement with model is only qualitative.

VI. DISCUSSION AND CONCLUSIONS

A computer was used in all routine phases of the experiment: control of measurement, data processing and storage and, finally, comparison with the experiment. Main computer use is in the device modeling. Models are based on the numeric integration that is relatively simple for programming, but time consuming at calculations. Thanks to very effective MATLAB processing of matrices, the numerical integration can be in principle performed at short times, at least for relatively simple models. Two devices were measured and modeled, the flow meter and distribution point. In the case of the flow meter the coil was modeled by its central conductor. Furthermore, geometrical details were not inserted into the wire geometry. Comparison of the experiment with this simple model is in good agreement from the technical point of view.

In principle the model can be improved if the 3D coil is considered and the geometry improved, but the computation time rapidly increases. Furthermore, the agreement will not be improved significantly, since we showed that the production and experimental inaccuracy play an important role.

Therefore, it is only an academic interest to improve the model, since it will be perfectly valid for only one realization of the device. Form of the practical point of the production inaccuracies view should be studied in the model and systematic experimental errors removed.

As for skin effect study we showed that for the given conductor geometry at the frequency of about 400 Hz the skin-effect takes a place theoretically. Its effect is not high; nevertheless, it was confirmed experimentally, but only qualitatively. Main problem is that the excitation current decreases with increasing frequency and magnetic field is low and difficult to measure. At the frequency of 1200 Hz the experimental errors are high.

Quantitative verification of the skin-effect formula (3) is limited by the low magnetic field that is difficult to measure precisely. Since the exciting current cannot be increased, the solution is to increase the probe sensitivity and accuracy and remove more effectively noise from data.

From the technical point of view good and reliable models are very important. If they are verified experimentally, they can be used to the optimum design of devices using the computer. The parameters of realization will be close to those obtained by calculations. Therefore, many expensive and time consuming experiments can be missed and the device will exhibit optimum parameters.

The use of the numeric integration is simple and leads to the same results as the famous finite element method. The numeric integration has a lot of advantages. The only disadvantage is its low speed. It was the reason, why we preferred the numeric integration approach in simple models.

ACKNOWLEDGMENT

This work was supported by Student grant TUL SGS 2012/7821 "Interactive mechatronics systems in technical cybernetics".

REFERENCES

- [1] T. Mikolanda, M. Košek., A. Richter, "3D magnetic field measurement, visualization and modelling," *In proc. of the 7th Intern. Conf. on Measurement*, 2009, pp. 306–309.
- [2] J.A. Shercliff, *The theory of electromagnetic flow-measurement.* Cambridge Science Classics – Cambridge University Press, Cambridge, 2009.
- [3] M. Košek, M. Truhlář, A. Richter, "Magnetic field of massive conductor at low frequency," *Electrical Review (Przegląd elektrotechniczny)*, vol. 88 NR 7a/2012, pp. 23–26, ISSN 0033-2097.
- [4] Frollo, P. Andris, J. Pribil, I. Vojtisek, Z. Holubekova, T. Dermek, "Magnetic field measurement of a planar coil using magnetic resonance imaging method," *In proc. of the 7th Intern. Conf. on Measurement*, 2009, pp. 238–240.
- [5] M. Novák, L. Slavík, M. Košek, M. Truhlář, "Measuring Low Magnetic Field in Electromagnetic Flow Meter," *In proc. of the 8th Intern. Conf. on Measurement*, 2011, pp. 245–248.